

NOTES AND CORRESPONDENCE

ECMWF and ERS-1 Surface Winds over the Arabian Sea during July 1995

DAVID HALPERN

Earth and Space Sciences Division, Jet Propulsion Laboratory, California Institute of Technology, Pasadena, California

MICHAEL H. FREILICH

College of Oceanic and Atmospheric Sciences, Oregon State University, Corvallis, Oregon

ROBERT A. WELLER

Department of Physical Oceanography, Woods Hole Oceanographic Institution, Woods Hole, Massachusetts

5 November 1997 and 10 September 1998

ABSTRACT

The European Centre for Medium-Range Weather Forecasts (ECMWF) and Institut Francais Pour la Recherche et l'Exploitation de la Mer European Remote-Sensing Satellite, named *IFR2*, surface wind velocity data products are compared during July 1995 over the Arabian Sea. Substantial differences were found. The central positions of the maximum isotach were separated by 450 km, and the ECMWF maximum isotach was 2 m s^{-1} higher than that of *IFR2*. *IFR2* wind components contained about 10 times more variance than ECMWF winds for horizontal distances from 50 to 250 km. Along the 8.5°N southern boundary of the Arabian Sea, ECMWF southward Ekman transport was higher than that of *IFR2* by an amount that could be observed with current measurements. The ECMWF and *IFR2* difference in upward transport of water into the Ekman layer, computed from wind stress curl, was large enough to measure.

1. Introduction

Surface wind velocity data products for the Arabian Sea are available from a variety of sources: wind reports from ships, operational wind field analyses produced at numerical weather prediction (NWP) centers, and wind velocity computed from satellite scatterometer measurements. Ship reports do not have uniform error characteristics and are highly aliased in time and space. The NWP data products suffer because of incomplete parameterizations of physical and thermodynamical processes and because of sparse distribution of ship wind observations used in data assimilation. Since the July 1991 launch of the first European Remote-Sensing Satellite (*ERS-1*), surface wind velocity fields have been created from scatterometer data.

This paper describes a comparison between *ERS-1 IFR2* (IFREMER 1996) and European Centre for Medium-Range Forecasts (ECMWF) 10-m height wind velocity

data products over the Arabian Sea for July 1995. We used the 6-h, $1.125^\circ \times 1.125^\circ$ ECMWF wind data product. The Institut Francais Pour la Recherche et l'Exploitation de la Mer (IFREMER) produced, in addition to *IFR2*, a version of the ECMWF wind product that was collocated with *IFR2* measurements (Anonymous 1996), which we named ECMWF/IFR. We chose July because it is climatologically the month with highest wind speeds (Hastenrath and Lamb 1979) and in July 1995 several international oceanographic field campaigns provide additional data.

In this report, the level of physical oceanographic significance between monthly mean wind speeds is 1 m s^{-1} . For oceanographic and meteorological conditions encountered at the Improved Meteorological (IMET) buoy (15.5°N , 61.5°E), where measurements of surface meteorological and upper-ocean variables had been recorded (Weller 1996), a $\pm 1 \text{ m s}^{-1}$ change in the 1-min wind speed measured during July 1995 corresponded to a net surface heat flux of $\pm 8 \text{ W m}^{-2}$. This value is about the precision required for studies of climate variability (Bretherton 1981).

2. Results

The patterns and general features of the July 1995 mean *IFR2*, ECMWF, and ECMWF/IFR wind velocities

Corresponding author address: Dr. David Halpern, Jet Propulsion Laboratory, MS 300-323, California Institute of Technology, 4800 Oak Grove Drive, Pasadena, CA 91109-8099.
E-mail: david.halpern@jpl.nasa.gov

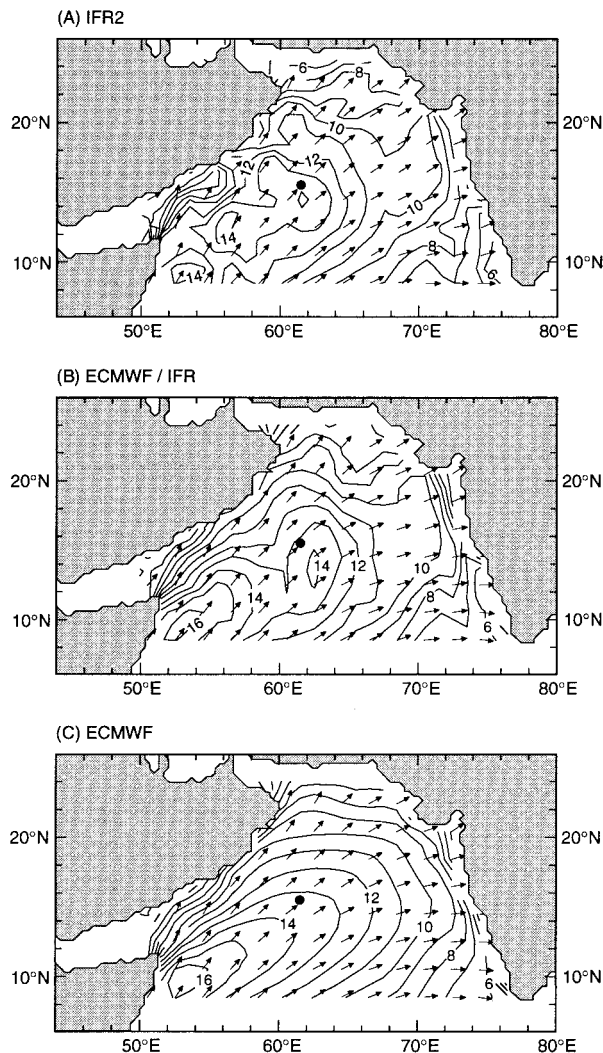


FIG. 1. Arabian Sea distributions of July 1995 scalar-averaged wind speed (contour interval = 1 m s^{-1}) and vector-averaged wind direction for (a) *IFR2*, (b) *ECMWF/IFR*, and (c) *ECMWF* data products. The dot at 15.5°N , 61.5°E represents the location of *IMET* wind observations.

over the Arabian Sea were qualitatively similar (Fig. 1). Boundaries of the Arabian Sea were arbitrarily defined to be 8.5°N , 24°N , 50°E , and 77°E . Distortions of the *ECMWF/IFR* isotachs compared to *ECMWF* (Figs. 1b and 1c) were introduced by the *ERS-1* scatterometer sampling scheme (Zeng and Levy 1995).

In July 1995 the location and magnitude of the maximum isotach varied with data product (Fig. 1). For *ECMWF* and *ECMWF/IFR*, the region of maximum isotach (16 m s^{-1}) was centered at 10°N , 53°E . The *ECMWF* and *ECMWF/IFR* maximum isotach was 2 m s^{-1} greater than the *IFR2* maximum isotach; the difference was twice the acceptable uncertainty. The *IFR2* data had three regions enclosed with the same maximum isotach (14 m s^{-1}), with the largest area centered at 13°N , 56°E . This site was 450 km northeast of the cen-

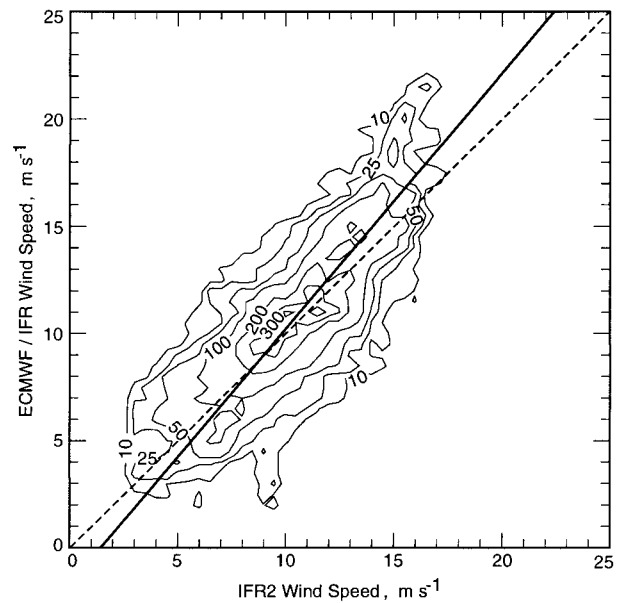


FIG. 2. Scatterplot of collocated *IFR2* and *ECMWF/IFR* wind speeds over the Arabian Sea during July 1995. Number of collocations was 45 363. Dash line represents perfect agreement. Solid line represents least-squares orthogonal regression line. Contours (with variable interval) are numbers of collocations.

ters of the *ECMWF* and *ECMWF/IFR* maximum isotach. Examination of Special Sensor Microwave/Imager wind speeds (Wentz 1997) showed that the position and magnitude of the maximum isotach (13 m s^{-1}) were more similar to those computed with *IFR2* data compared to *ECMWF* data.

a. Regression analysis

For *IFR2* speeds below (above) 8.7 m s^{-1} , *ECMWF/IFR* speeds were lower (higher) than *IFR2* speeds (Fig. 2). For *IFR2* speeds between 3 and 14 m s^{-1} , the regression line was within 1 m s^{-1} of the 1:1 line of perfect correspondence. For *IFR2* speeds greater than 15 m s^{-1} , the predicted residual speed between *ECMWF/IFR* and *IFR2* was greater than 1 m s^{-1} . The correlation coefficient between *ECMWF/IFR* and *IFR2* wind speeds was 0.8 , which was significant at the 95% confidence level. In this report, the level of statistical significance is 95%. Large differences between collocated *ECMWF/IFR* and *IFR2* speeds yielded a rms difference of 2.1 m s^{-1} , which was twice the desired level of uncertainty.

b. Temporal variability

The July 1995 *ECMWF/IFR* and *IFR2* $1^\circ \times 1^\circ$ wind speed variances averaged over the Arabian Sea were 4.8 and $3.6 \text{ m}^2 \text{ s}^{-2}$, respectively, which were significantly different according to the *F* test. To examine the representativeness of the *ECMWF* temporal structure, 6-h *ECMWF* and *IMET* data were compared for July 1995.

IMET data were averaged over 6 hours centered on the ECMWF forecast time. The ECMWF and IMET July 1995 mean wind speed difference was less than 1 m s^{-1} . However, the ECMWF u variance ($3.3 \text{ m}^2 \text{ s}^{-2}$) and v variance ($4.1 \text{ m}^2 \text{ s}^{-2}$) were nearly two and three times, respectively, greater than the corresponding IMET variances. The differences between the ECMWF and *IFR2* wind component variances were significant.

Spectra of ECMWF and IMET u and v components yielded the distribution of variance with frequency (Fig. 3). In contrast to the large difference in IMET u spectral levels between low and high frequencies, the ECMWF u spectrum was almost flat. At the diurnal frequency and at higher frequencies, the ECMWF u spectral values were significantly different. Significant statistical difference of spectral estimates means that confidence intervals associated with ECMWF and *IFR2* spectral values at the same frequency did not overlap. In the ECMWF v component, the amplitude of the diurnal-period oscillation was significant. At the diurnal period, the ECMWF rms wind speed amplitude (0.8 m s^{-1}) was 2.7 times greater than that computed with IMET data.

We did not expect ECMWF data to have more temporal variability than IMET data. In the ECMWF forecast-analysis system, data gaps of the surface wind field to be ingested into the atmosphere model were filled with previous forecasts, which should reduce temporal variability.

c. Spatial variability

The *IFR2* data occurred along 19 cell tracks parallel to the *ERS-1* ground track. During July 1995, there were 102 cell tracks, each with 72 25-km elements, in the region bounded by $56^\circ\text{--}70^\circ\text{E}$ along 8°N and by $60^\circ\text{--}68^\circ\text{E}$ along 24°N . The 6-h ECMWF data between 8° and 24°N were interpolated to 72 24.4-km intervals along five meridians ($61^\circ, 62^\circ, 63^\circ, 64^\circ,$ and 65°E). Before computing the periodogram, the u and v components along each cell track (for *IFR2*) and meridian (for ECMWF) were prewhitened to reduce spectral leakage. For *IFR2*, the spectral estimate for each wave number k_i was equal to the arithmetic mean value of the 102 recolored periodogram ordinates at k_i . For ECMWF, spectral estimates were computed from 124 periodograms along each meridian, and then the five-meridian average spectra were computed. For ECMWF spectra, confidence limits are not easily determined because each 6-h wind field was not an independent representation of the wind field. We arbitrarily allow the ECMWF-spectral confidence intervals to equal that corresponding to 204 degrees of freedom, instead of 1240 degrees of freedom had each ECMWF wind field been independent.

For wave lengths smaller than 400 km, *IFR2* u - and v -spectral estimates were significantly larger than ECMWF with differences increasing from one-third at 400 km to nearly 100 at 50 km (Fig. 4). Stoffelen (1998)

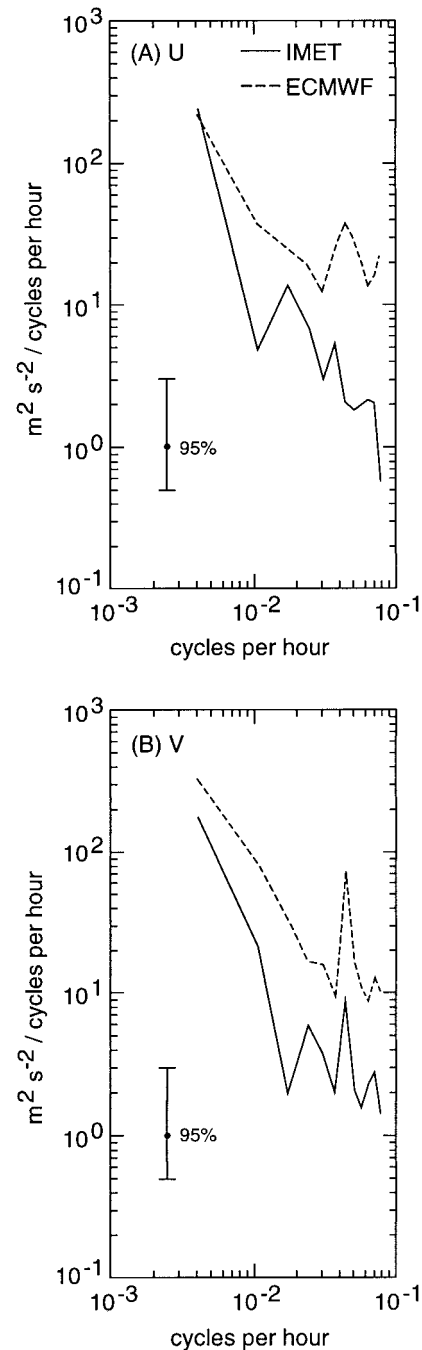


FIG. 3. Frequency spectra of (a) east-west, u , and (b) north-south, v , wind velocity components for IMET and ECMWF data during July 1995. The 95% represents the 95% confidence levels determined from the chi-square distribution.

reported that *ERS-1* winds, which had been computed with an algorithm different than the one we used, contained substantially more variance than ECMWF winds on scales between 50 and 250 km. It is not surprising that ECMWF data have lower variability in space compared to *IFR2* because the ECMWF assimilation scheme

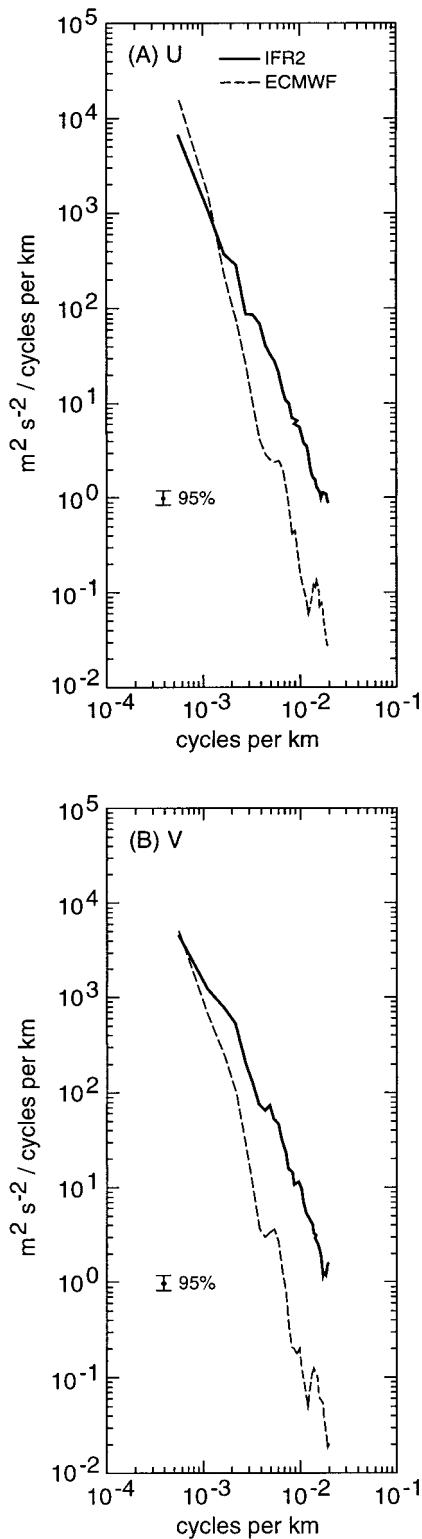


FIG. 4. Wavenumber spectra of (a) east–west, u , and (b) north–south, v , wind velocity components for ECMWF and *IFR2* data during July 1995 in the central Arabian Sea. The 95% represents the 95% confidence levels determined from the chi-square distribution.

used a weighted average of all data less than 3 h apart from the 6-h forecast verification time and over a 500-km region. This is in marked contrast to the instantaneity and 50-km resolution of *IFR2* data.

The ECMWF u - and v -spectra displayed significant peaks of approximately equal amplitude at 64 km; the *IFR2* spectra contained no such spectral peak (Fig. 4). The variance at 64 km was 10^4 times smaller than that at 1000 km. No hypothesis nor previous observation justify a spectral peak at 64 km, indicating that the small-amplitude spectral peak is spurious.

Throughout the 1800- to 50-km range, the *IFR2* u - and v -spectral (log–log) slopes were -2.6 and -2.4 , respectively (Fig. 4), which were nearly 25% greater than those computed by Freilich and Chelton (1986) for the trade wind zone in the Pacific Ocean.

d. Wind-driven ocean transports

Employing conservation of mass, a lowest-order approximation of Arabian Sea southwest monsoon wind-driven ocean circulation is meridional flow across the southern boundary at 8.5°N , vertical exchange between the thermocline and near-surface layers, and water entering the Arabian Sea by the narrow Somali Current. Attention is focused on Ekman transport and upward transport into the near-surface layer, which were computed by methods described in Halpern et al. (1998).

Along the Arabian Sea southern boundary at 8.5°N , the integrated southward Ekman transports in July 1995 for ECMWF, ECMWF/*IFR2*, and *IFR2* were -17.5 , -16.7 , and -12.5 Sv ($\text{Sv} \equiv 10^6 \text{ m}^3 \text{ s}^{-1}$), respectively. The 4.2 Sv difference between ECMWF/*IFR2* and *IFR2* would correspond to a southward Ekman current averaged over 50 m of 3 cm s^{-1} , which is a measurable quantity.

The July 1995 ECMWF, ECMWF/*IFR2*, and *IFR2* vertical transports into the Ekman layer integrated over the Arabian Sea north of 8°N were 6.3, 5.2, and 3.2 Sv, respectively. The 2 Sv (or 48%) difference between ECMWF/*IFR2* and *IFR2* corresponded to an average vertical velocity uncertainty of $0.6 \times 10^{-6} \text{ m s}^{-1}$. This value is comparable to the error associated with vertical velocity estimated from the continuity equation and horizontal current measurements. North of 13°N where vertical motion was upward, the average difference between ECMWF/*IFR2* and *IFR2* vertical velocities was $1.8 \times 10^{-6} \text{ m s}^{-1}$ or three times greater than the average over the Arabian Sea.

3. Concluding remarks

Results included 1) ECMWF/*IFR2* wind speeds were greater (smaller) than *IFR2* at high (low) wind speeds; 2) *IFR2* maximum isotach (14 m s^{-1}) was centered 450 km toward the northeast and was 2 m s^{-1} smaller compared to ECMWF maximum isotach (wind speed differences greater than 1 m s^{-1} were significant); 3) at all

frequencies (1.34×10^{-3} – 8.33×10^{-2} cycles per hour) ECMWF wind component spectral values were greater than those computed from moored-buoy wind observations at 15.5°N , 61.5°E , and at the diurnal period the ECMWF wind speed amplitude was nearly three times greater than that computed with wind recorder data; 4) zonal and meridional spectral values of ECMWF motions were significantly smaller than *IFR2* for horizontal scales from 400 to 50 km; 5) *IFR2* southward Ekman transport integrated along 8.5°N was substantially greater than that computed with ECMWF data; and 6) upward transport of water into the Ekman layer over the Arabian Sea was less for *IFR2* than ECMWF, especially over the northern Arabian Sea.

Studies of wind-driven ocean circulation, especially those related to monsoon dynamics of the Arabian Sea, require accurate winds. Local wind-driven velocities, away from the coast, are essentially linearly related, at each frequency, to the wind stress (Weller 1981), and the higher ECMWF energy levels (Fig. 3) would result in stronger wind-driven currents and shear at the base of the mixed layer compared to *IFR2*. ECMWF southward Ekman transport and upward transport into the Ekman layer would yield stronger meridional overturning circulation in the north Indian Ocean compared to *IFR2*. Further studies are warranted with other NWP wind products, as well as numerical simulations utilizing these products.

Acknowledgments. We are extremely grateful to the IFREMER Centre ERS d'Archivage et de Traitement (CERSAT) for producing and distributing ECMWF/IFR and IFR2 data. Dr. Frank Wentz (Remote Sensing Systems) kindly provided SSMI winds for July 1995. The manuscript benefited greatly from constructive comments by Dr. Craig Lee (WHOI), Dr. Ad Stoffelen (KNMI), and two anonymous reviewers. Data process-

ing and graphics were made by Peter Woiceshyn (JPL) in his usual proficient manner. The work described in this paper was supported by NASA 622-47-09 (DH), NASA SeaWinds Project 229-18-41 (DH), NASA NSCAT Project via JPL Contract 959351 (MHF), and ONR Grant N00014-94-1-0161 (RW). The research described in this paper was performed, in part, by the Jet Propulsion Laboratory, California Institute of Technology, under contract with the National Aeronautics and Space Administration.

REFERENCES

- Bretherton, F., 1981: The ocean surface energetics—A need for climate understanding. *Applications of Existing Satellite Data to the Study of the Ocean Surface Energetics*, C. Gautier, Ed., University of Wisconsin Press, 5–14.
- Freilich, M. H., and D. B. Chelton, 1986: Wavenumber spectra of Pacific winds measured by the Seasat scatterometer. *J. Phys. Oceanogr.*, **16**, 741–757.
- Halpern, D., M. H. Freilich, and R. A. Weller, 1998: Arabian Sea surface winds and ocean transports determined from *ERS-1* scatterometer. *J. Geophys. Res.*, **103**, 7799–7805.
- Hastenrath, S., and P. J. Lamb, 1979: *Climatic Atlas of the Indian Ocean*. University of Wisconsin Press, 19 pp and 97 charts.
- IFREMER, 1996: Off-line wind scatterometer ERS products—Users' manual. CERSAT Ref. C2-MUT-W-01-IF: V2.0, Dept. Ocean. from Space, IFREMER, Plouzane, France, 85 pp. [Available from IFREMER, B.P. 70, 29280 Plouzane, France.]
- Stoffelen, A., 1998: Towards the true near surface wind speed: Error modeling and calibration using triple collocation. *J. Geophys. Res.*, **103**, 7755–7766.
- Weller, R. A., 1996: In situ observations of surface meteorology and air–sea fluxes. 1996 U.S. WOCE Implementation Rep. 8, 48 pp. [Available from the Department of Oceanography, Texas A&M University, College Station, TX 77843.]
- , 1981: Observations of the velocity response to wind forcing in the upper ocean. *J. Geophys. Res.*, **86**, 1969–1977.
- Wentz, F. J., 1997: A well-calibrated ocean algorithm for special sensor microwave/imager. *J. Geophys. Res.*, **102**, 8703–8718.
- Zeng, L., and G. Levy, 1995: Space and time aliasing structure in monthly mean polar-orbiting satellite data. *J. Geophys. Res.*, **100**, 5133–5142.